Optical images of the 3D microvascular network were captured by a Canon 141 Digital Camera (Canon U.S.A, Inc., Lake Success, NY). Fluorescence microscope images were obtained with a Zeiss Axiovert 100 fluorescence light microscope (Carl Zeiss Microimaging, Thornwood, NY) with a 2.5 × objective.

Received: March 29, 2004
Final version: October 15, 2004

[1] a) A. Strömberg, A. Karisson, F. Ryttsén, M. Davidson, D. T. Chiu, O. Orwar, *Anal. Chem.* **2001**, *73*, 126. b) H.-P. Chou, C. Spence, A. Scherer, S. Quake, *Proc. Natl. Acad. Sci. U. S. A.* **1999**, *96*, 11.

[2] a) G. J. Snyder, J. R. Lim, C.-K. Huang, J.-P. Fleurial, *Nat. Mater.* **2003**, *2*, 528. b) Y. Mizukami, D. Rajniak, A. Rajniak, M. Nishimura, *Sens. Actuators, B* **2002**, *81*, 2002.

[3] a) M. L. Chabinyc, D. T. Chiu, J. C. McDonald, A. D. Stroock, J. F. Christian, A. M. Karger, G. M. Whitesides, *Anal. Chem.* **2001**, *73*, 4491. b) A. E. Kamholz, B. H. Weigl, B. A. Finlayson, P. Yager, *Anal. Chem.* **1999**, *71*, 5340. c) J.-C. Roulet, R. Völkel, H. P. Herzig, E. Verpoorte, N. F. de Rooij, R. Dändliker, *J. Microelectromech. Syst.* **2001**, *10*, 1057.

[4] a) M. W. Losey, M. A. Schmidt, K. F. Jensen, *Ind. Eng. Chem. Res.* **2001**, *40*, 2555. b) S. K. W. Dertinger, D. T. Chiu, N. L. Jeon, G. M. Whitesides, *Anal. Chem.* **2001**, *73*, 1240.

[5] a) S. R. White, N. R. Sottos, P. H. Geubelle, J. S. Moore, M. R. Kessler, S. R. Sriram, E. N. Brown, S. Viswanathan, *Nature* **2001**, *409*, 794. b) D. J. Beebe, J. S. Moore, J. M. Bauer, Q. Yu, R. H. Liu, C. Devadoss, B.-H. Jo, *Nature* **2000**, *404*, 588.

[6] a) D. J. Beebe, J. S. Moore, Q. Yu, R. H. Liu, M. L. Kraft, B.-H. Jo, C. Devadoss, *Proc. Natl. Acad. Sci. U. S. A.* **2000**, *97*, 13 488. b) J. C. McDonald, D. C. Duffy, J. R. Anderson, D. T. Chiu, H. Wu, O. J. A. Schueller, G. M. Whitesides, *Electrophoresis* **2000**, *21*, 27.

[7] a) D. Therriault, S. R. White, J. A. Lewis, *Nat. Mater.* **2003**, *2*, 265. b) S. J. Qin, W. J. Li, *Sens. Actuators, A* **2002**, *97–98*, 749. c) J. C. McDonald, M. L. Chabinyc, S. J. Metallo, J. R. Anderson, A. D. Stroock, G. M. Whitesides, *Anal. Chem.* **2002**, *74*, 1537. d) H. Wu, T. W. Odom, D. T. Chiu, G. M. Whitesides, *J. Am. Chem. Soc.* **2003**, *125*, 554. e) J. R. Anderson, D. T. Chiu, R. J. Jackman, O. Cherniavskaya, J. C. McDonald, H. Wu, S. H. Whitesides, G. M. Whitesides, *Anal. Chem.* **2000**, *72*, 3158. f) B.-H. Jo, L. M. van Lerberghe, K. M. Motsegood, D. J. Beebe, *J. Microelectromech. Syst.* **2000**, *9*, 76.

[8] a) J. Cesarano III, P. D. Calvert, *US Patent 6 027 326*, **2000**. b) Q. Li, J. A. Lewis, *Adv. Mater.* **2003**, *15*, 1639. c) J. E. Smay, J. Cesarano III, J. A. Lewis, *Langmuir* **2002**, *18*, 5429. d) J. E. Smay, G. M. Gratson, R. F. Sheperd, J. Cesarano III, J. A. Lewis, *Adv. Mater.* **2002**, *14*, 1279.

[9] D. Therrriault, *Ph.D. Thesis*, University of Illinois at Urbana-Champaign **2003**.

Bioactive Hydrogels with an Ordered Cellular Structure Combine Interconnected Macroporosity and Robust Mechanical Properties**

By *Agnieszka N. Stachowiak*, *Anna Bershteyn*, *Elina Tzatzalos*, and *Darrell J. Irvine**

Bioactive hydrogels that consist of a cellular structure of interconnecting macropores combine tissue-like elasticity with enhanced pathways for mass transport and cell migration, making them attractive scaffolds for drug delivery and tissue engineering.[1–4] However, in order to obtain high degrees of pore interconnectivity using available stochastic porogen methods, void fractions exceeding 95 % must be introduced,[5–8] severely impacting mechanical properties such that a limited selection of stiff materials can be utilized.[3,9] Here we report a method to prepare soft hydrogels with interconnected porosity at moderate void fractions, thus maintaining a compressive stiffness that is comparable to native tissues. This was achieved by fabricating gels with ordered, interconnected macrovoids (20–60 μm diameter) via colloidal-crystal templating. The templated bioactive hydrogels supported cell attachment and migration through the interconnected structure. Two ubiquitous biomaterials, crosslinked poly(ethylene glycol) and gelatin, were templated; the generality of the approach should make it applicable to materials of interest for a broad range of bioengineering applications.

Colloidal-crystal templating has been extensively applied for the fabrication of photonic crystals, membranes, chromatography media, and solid-phase catalysis substrates.[10–13] The template is comprised of a crystalline arrangement of monodisperse microspheres (typically silica or polystyrene), which can

[*] Prof. D. J. Irvine, A. N. Stachowiak, A. Bershteyn
Department of Materials Science & Engineering
Massachusetts Institute of Technology
Cambridge, MA 02139 (USA)
E-mail: djirvine@mit.edu
Prof. D. J. Irvine
Biological Engineering Division
Massachusetts Institute of Technology
Cambridge, MA 02139 (USA)
E. Tzatzalos
Department of Chemical Engineering
Massachusetts Institute of Technology
MIT Room 8–425
77 Massachusetts Ave.
Cambridge, MA 02139 (USA)

[**] This work was supported by the Whitaker Foundation (grant number RG-02-0837). AS was supported by a National Defense Science and Engineering Graduate fellowship. We thank Lorna Gibson, Don Galler, Brendan Harley, and Nicki Watson (Keck Imaging Facility, Whitehead Institute) for helpful discussions. Supporting Information is available online from Wiley InterScience, or from the authors.

 DOI: 10.1002/adma.200400507

ADVANCED MATERIALS

be used as an extractable template for the fabrication of inorganic materials, metals, or polymers with close-packed voids of ~0.05–5 μm diameter (commonly referred to as inverse opal structures). In order to adapt colloidal-crystaltemplating to the fabrication of tissue-engineering scaffolds, we prepared 1–2 mm thick templates from monodisperse polymer microspheres with 20–60 μm diameters. Colloidal crystal templates (CCTs) can be prepared from submicrometer-diameter particle suspensions simply by controlled evaporation, with random thermal motion enabling the spheres to evolve to close-packed structures as they are concentrated.[11,12] For the large microspheres used in our templates, Brownian forces were insufficient to promote ordering; we previously reported that controlled evaporation alone does not lead to close packing of large microspheres (resulting in imperfect templated gel structures).[14] To overcome this problem, and achieve highly ordered CCTs, we incubated drying samples atop a reciprocating shaker.

We first templated synthetic hydrogels based on cross-linked poly(ethylene glycol) (PEG), a common tissue engineering matrix material (Fig. 1a).[1,15–17] Hydrogel precursor solution was perfused through the template by centrifugation and subsequently photopolymerized, after which the template was removed by solvent extraction. The morphology of the resulting templated hydrogels was characterized by optical, fluorescence, and scanning electron microscopy (SEM). As shown in Figures 1b,c (top), scaffolds examined in the hydrated state exhibited a cellular structure with long-range hexagonally close-packed order; cell size was exactly dictated by the diameter of the templating microspheres. Regions of sphere–sphere contact in the original template created ordered arrays of intercell pores, as illustrated by three-dimensional (3D) reconstructions of serial confocal images through a scaffold layer (Fig. 1c, bottom); scaffolds typically had ~78 % of the pores expected for a perfect structure (determined from 3D confocal data), which is well above the threshold for a fully percolating structure.[18,19]

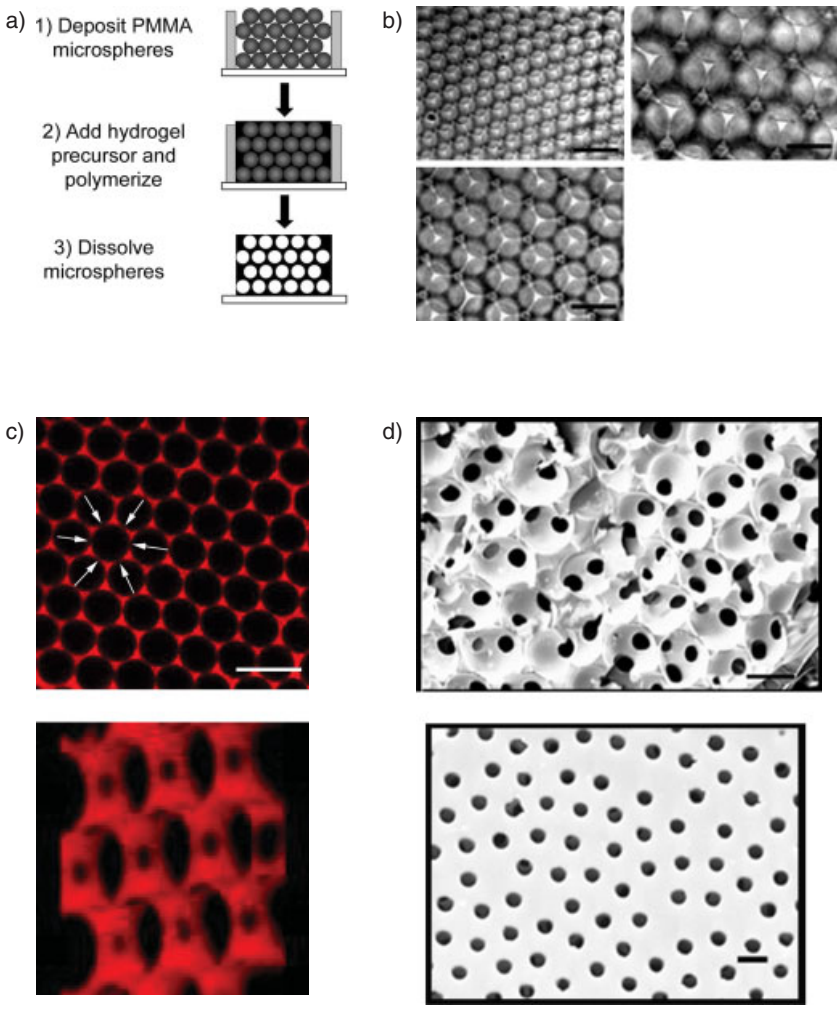

Figure 1. Scaffold fabrication and morphology. a) Schematic of hydrogel templating process. b) Bright-field optical micrographs taken within hydrated PEG gels templated with 20, 40, or 60 μm diameter microspheres (scale bars 50 μm). c) (Top) Confocal image of a fluorescently labeled, hydrated PEG scaffold taken through the mid-plane of a single layer within the structure (scale bar 40 μm). Scaffolds with 20 μm cells had 65 ± 3 % porosity (determined from intensity-thresholded 3D confocal data). Breaks in fluorescence intensity around each cell of the structure occur at open inter-cell pores (denoted for one cell with arrows). (Bottom) A 3D reconstruction of serial *z*-section confocal images taken in 0.5 μm steps shows the lateral intercell pores formed at points of sphere–sphere contact in the colloidal crystal template: a small section of one scaffold layer is shown at a 135° angle. d) SEM images of dehydrated scaffolds: (Top) Cross-sectional image taken near the center of a templated scaffold. Gels exhibited cell ordering and interconnectivity throughout their cross-sections (scale bar 50 μm, corrected for shrinkage due to dehydration; 28 μm uncorrected). (Bottom) Templated hydrogels also exhibited porosity at their free surfaces, as illustrated by this scaffold with a 20 μm cell size (scale bar 20 μm, corrected).

To probe morphology within the center of millimeter-thick structures, dehydrated scaffolds were also examined by SEM. Upon dehydration, scaffolds shrank by ~40 %, but did so uniformly (Fig. 1d, top). Gels exhibited ordered cells and cell–cell connectivity throughout their cross-sections. Templated scaffolds with 40 μm or greater cell size had intercell pore diameters ≥10 μm, consistent with those reported to support tissue invasion in vivo (Table 1).[20–22] In addition, while some stochastic porogen methods used for the fabrication of tissue engineering scaffolds create dense or nonporous skin layers which may block entry of cells into implanted structures,[23,24] templated gels had well-defined porosity at their free surfaces (Fig. 1d, bottom).

Table 1. Templated PEG scaffold pore sizes and compressive moduli.

Nominal cell size [μm]	Dehydrated inter-cell pore diameter [μm]	Inter-cell pore diameter, corrected [μm] [a]	No. pores examined	Compressive modulus [kPa] [b]
20	2.94 ± 0.57	5.15 ± 1.00	53	16.0 ± 4.3
40	5.53 ± 0.87	9.67 ± 1.53	111	18.0 ± 4.2
60	8.86 ± 1.81	15.5 ± 3.17	116	22.6 ± 5.0

[a] Intercell pore size determined from SEM images of scaffolds was corrected by dividing by the fractional shrinkage observed in the dehydrated structure relative to the dimensions of the hydrated scaffold measured in situ by confocal microscopy.
[b] Modulus of non-templated PEG hydrogel was 160 ± 53 kPa.

The high degree of cell interconnectivity observed in templated gels was achieved at significantly lower total porosities than were required in stochastic porogen methods due to the ordered arrangement of void space, and this resulted in improved mechanical properties. Using a model of bending response in porous structures, Gibson and Ashby derived a relationship between the elastic modulus of cellular materials (E_{cellular}) and their solid counterparts (E_{solid})[25]

$$\frac{E_{\text{cellular}}}{E_{\text{solid}}} = C(1-P)^2 \quad (1)$$

where C is a constant (typically ≈ 1) and P is the porosity. Equation 1 predicts the modulus of structures with 95–99 % porosity to be 0.25 %–0.01 % of the bulk solid, in agreement with reported data on tissue engineering scaffolds.[6–8] Such porosity levels lead to extremely low moduli for soft hydrogel structures, and therefore prior studies of macroporous soft gels have typically been confined to small cell sizes[4,26] (≤ 15 μm) and/or to low total porosities (≤ 35 %).[27,28] Compressive moduli of our templated PEG hydrogels in the hydrated state were found to be comparable to soft tissues, which range from ~ 1 to a few tens of kilopascals (Table 1).[29,30] In agreement with Equation 1, our data yielded a value of $E_{\text{templated}}/E_{\text{solid}} = 0.120 \pm 0.05$ for the PEG hydrogels, versus 0.108 predicted for close-packed void structures with maximal theoretical porosity (74 %). Thus, the templated structure combines excellent cell interconnectivity with relative stiffnesses ten to one-thousand-fold greater than those predicted for disordered structures, where high porosity is a prerequisite for high interconnectivity ($E_{74\ \%\ \text{porous}}/E_{99\ \%\ \text{porous}} \approx 676$).

We next examined cell attachment and migration in templated bioactive PEG hydrogels by three-dimensional epifluorescence microscopy. PEG networks are readily functionalized with short peptides that support cell adhesion via specific integrin cell surface receptors.[1,15,17] PEG monoacrylates conjugated with the adhesion peptide Gly–Trp–Gly–Arg–Gly–Asp–Ser–Pro (GWGRGDSP)[31] (RGD-PEGA) were synthesized, which provided RGD-mediated cell attachment to PEG hydrogels for at least 12 h (data not shown).[32] Others have reported potential issues with protein adsorption to low-molecular-weight PEG gels.[33,34] However, hydrogels with bulk compressive moduli in the range of 10–100 kPa may be prepared from higher molecular weight PEGs, suggesting that this templating approach could be readily applied to such gels.[35,36]

As illustrated in Figure 2a, mouse NR6 fibroblasts were able to attach and spread inside RGD-modified scaffolds over at least several days when cultured within scaffolds in vitro. Further, loading of RGD-functionalized scaffolds with highly motile cells (T cell clones or primary T cells isolated from lymph nodes of OT-II mice) showed that the interconnecting pores readily supported cell migration throughout the matrices in three dimensions (illustrated by the time-lapse images shown in Figure 2b; see also Supporting Information). Thus the connected cellular structure of templated gels provided functional pathways for cell migration within the scaffold.

In addition to functionalization by short peptide ligands, the interconnected porosity of the templated structure makes post-synthesis functionalization of all interior surfaces of the gel with intact extracellular matrix (ECM) proteins possible

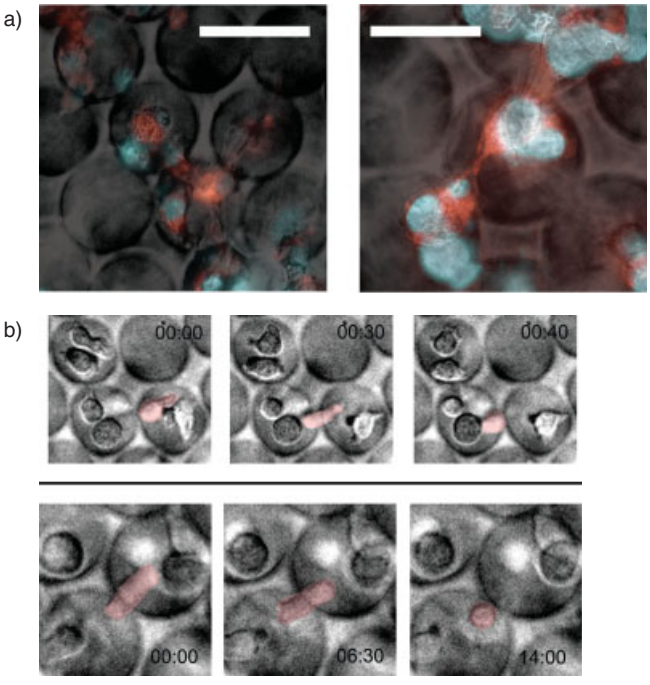

Figure 2. Cell attachment and migration in templated PEG hydrogels. a) Overlaid bright-field optical and fluorescence micrographs of stained NR6 fibroblasts spread on RGD-functionalized PEG scaffolds with 40 (left) and 60 (right) μm void sizes, after 24 h (scale bars 50 μm). Fluorescence staining of cells within scaffold: red, PKH26 membrane dye, blue, DAPI nuclear stain. b) Time-lapse bright-field optical microscopy images of T lymphocytes migrating through intercell pores in scaffolds. Primary T cells isolated from OT-II mice (top) and D10 $CD4^+$ T cell clone (bottom) are shown migrating in scaffolds with 20 and 30 μm voids, respectively. Times are elapsed minutes:seconds; the cell of interest in each case has been identified with a false-color overlay. (See Supplementary Information for Quicktime movies of these time-lapse images).

ADVANCED MATERIALS

by simply incubating the templated macroporous gel in a solution of protein which can react with functional groups present on the gel surfaces; we demonstrated this by coupling biotinylated fibronectin to biotinylated PEG scaffolds via a streptavidin bridge (data not shown).

An attractive feature of the colloidal-crystal templating approach is its potentially broad applicability for scaffold fabrication; any aqueous solution undergoing a permanent liquid–to–solid transition can in principle be templated with an ordered microstructure. To demonstrate this, we also templated the biological hydrogel formed by gelatin. This was done by introducing the heated gelatin solution into a colloidal template in the same way as for the synthetic PEG hydrogels, and solidifying the solution by cooling (followed by carbodiimide crosslinking). Gelatin hydrogels prepared in this manner were examined by optical and electron microscopy. Upon extraction of the templating microspheres, an ordered gelatin scaffold with interconnecting pores remained, as shown in the bright-field and electron micrographs of Figure 3. Intercell pore diameters were consistently ~40 % of the nominal pore diameter (cf. ~25 % for PEG gels), thus creating large pathways for cell migration even at the minimum 20 μm void diameter, as shown in Table 2. Acetic acid treatment of the gelatin scaffolds did not negatively impact cell attachment to the templated scaffolds. Primary T cells and NR6 fibroblasts attached and migrated within the ECM scaffolds as in the RGD-PEG scaffolds (data not shown). Compressive moduli of gelatin scaffolds were determined as for the PEG gels, and mechanical properties, though reduced, remained suitable for mimicking soft tissues (Table 2). Further, the decrease in modulus from bulk to porous gelatin was again consistent with the Gibson–Ashby theory, since $E_{templated}/E_{solid} = 0.100 \pm 0.026$. Similar fabrication approaches should make the colloidal crystal templating technique applicable to a variety of biomaterials.

Table 2. Templated gelatin scaffold pore sizes and compressive moduli.

Nominal cell size [μm]	Inter-cell pore diameter [μm]	No. pores examined	Compressive modulus [kPa] [a]
20	8.82 ± 2.66	54	3.1 ± 0.7
40	16.7 ± 4.28	49	3.3 ± 1.7
60	21.8 ± 5.50	50	5.0 ± 2.5

[a] Modulus of non-templated gelatin was 37.5 ± 13.7 kPa.

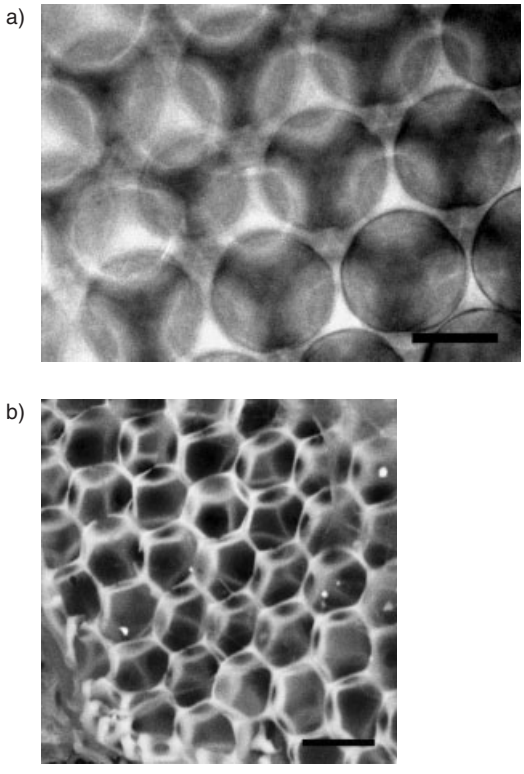

Figure 3. ECM-based templated hydrogels. a) Brightfield optical micrograph of hydrated gelatin scaffold templated with 60 μm diameter microspheres (scale bar 40 μm). b) SEM image of freeze-fractured gelatin scaffold with 20 μm cell size (scale bar 40 μm).

In summary, we have introduced a novel method for preparing bioactive scaffolds with ordered, highly interconnected macroporosity, and shown its applicability to two widely used hydrogel biomaterials. Using this approach, the attractive properties of hydrogels, such as biochemical versatility, tissue-mimetic mechanical properties, and hydrophilicity, may be combined with the benefits of an interconnected macroporous structure, including improved nutrient transport, space for cell migration, and fidelity to reticular ECM structures found in tissues such as bone marrow, lymph nodes, and the spleen.[37,38]

Experimental

Preparation of Colloidal Crystal Templates: A suspension of monodisperse poly(methyl methacrylate) (PMMA) microspheres (Fluka, 40 % solids in 30:70 vol:vol water/ethanol) was deposited in 4.8 mm diameter poly(dimethyl siloxane) wells adhered to glass slides, and dried atop a reciprocating shaker operated at 250 rpm for 4 h at 20 °C.

Preparation of PEG Scaffolds: A hydrogel precursor solution was prepared containing 20 % (*w*/*v*) PEG dimethacrylate (PEGDMA, Polysciences, MW = 1000 g mol^{-1}), 0.15 M triethanollamine, and 0.8 % hexyl phenyl ketone photoinitiator in 3:1 (*v*/*v*) 4-(2-hydroxyethyl)piperazine-1-ethanesulfonic acid (HEPES)-buffered saline pH 7.4 and ethanol. The precursor (12 μL) was gently pipetted onto the template, perfused by centrifugation (3 min, 1500 rpm), and exposed to UV light (365 nm, 12 mW cm^{-2}) for 90 s in order to polymerize the diacrylate. The polymerized construct was transferred to acetic acid in order to dissolve the microspheres over 48 h, and finally equilibrated in sterile phosphate-buffered saline pH 7.4.

Preparation of Functional PEG Scaffolds: Fluorescent scaffolds were prepared by including 0.003 wt.-% Fluor 570 methacrylate (Polysciences, Inc.) in the gel precursor solution. To prepare bioactive scaffolds, hydrogel precursor solution containing 1:160 mol:mol RGD-PEGA/PEGDMA was polymerized around colloidal crystal templates as before. Peptide-modified PEG acrylates (RGD-PEGA) were prepared by reacting 0.5 molar excess acryloyl-PEG-*N*-hydroxysuccinimide (PEGA-NHS, Nektar, MW = 3400 Da) with the adhesion

peptide [31] GWGRGDSP or a control peptide GWGR*DG*SP (MIT Biopolymers Laboratory) in pH 8.3 sodium bicarbonate buffer for 2 h at 20 °C, then dialyzing to remove excess PEGA-NHS (3500 MW cutoff, Pierce) [39].

Preparation of Scaffolds for SEM: PEG scaffolds were serially dehydrated (10, 25, 50, and 75 % ethanol at 10 min each; 100 % overnight), razor-cut, and observed using a LEO VP-438 at 5 kV. Gelatin scaffolds were frozen in liquid nitrogen, fractured, and lyophilized for 24 h prior to observation with a LEO VP-438, which was used in variable pressure mode (20 Pa) at 20 kV.

Confocal Microscopy: Fluorescent scaffolds were observed using a Zeiss LSM 510 with 40X Apochromat water-corrected objective.

Mechanical Properties Testing: Compressive moduli of hydrated PEG and gelatin scaffolds were measured at a constant strain rate (5 $\mu m\,s^{-1}$) using a precision motor stage (Micromechanics, UK) and a 25 g load cell (Transducer Techniques, CA). Data is reported as mean ± standard error.

Cell Culture: NR6 fibroblasts were the gift of Dr. Douglas Lauffenburger, and were cultured in Dulbecco's Modified Eagle's medium. OT-II T cells were derived from the lymph nodes of OT-II transgenic mice (Jackson Laboratories) and cultured in RPMI 1640. D10 T cells were a gift of Dr. Mark Davis and cultured in RPMI 1640. All media were supplemented with 10 % fetal calf serum, antibiotics, sodium pyruvate, non-essential amino acids, and 10 mM HEPES.

Cell Loading and Observation in Scaffolds: Fibroblasts or T cells were seeded by adding 10^6 cells in 20 μL RPMI medium to a scaffold, and incubating at 37 °C with shaking for 15 min. NR6 fibroblasts were treated with PKH26 membrane dye (Sigma) prior to loading, and with DAPI nuclear stain (Molecular Probes) at least 24 h after loading, according to manufacturer's instructions. Cells were observed using a Zeiss Axiovert 3D epifluorescence microscope equipped with piezoelectric objective *z* positioner and environmental stage (37 °C, 5 % CO_2), with the aid of Metamorph software.

Preparation of Gelatin Scaffolds: PMMA templates were heated to 70 °C and pre-wet with 70 % ethanol, after which gelatin solution at 70 °C (Sigma Type A, ~300 Bloom, 200 $mg\,mL^{-1}$, prepared in 25 % aqueous ethanol) was immediately added and perfused by centrifugation (5 min, 2000 rpm, 30 °C). After cooling to room temperature for 30 min, gels were flash frozen in liquid nitrogen and lyophilized overnight. Dehydrated gels were then treated with carbodiimide (0.20 mM *N*-Ethyl-*N*′-(3-dimethylaminopropyl)carbodiimide and 0.07 mM *N*-hydroxysuccinimide for 3 h at 20 °C) to form covalent cross-links that remain stable during template dissolution [40]. After the PMMA template was dissolved in acetic acid, the construct was rinsed and equilibrated in PBS pH 7.4.

Received: April 5, 2004
Final version: June 18, 2004
Published online: November 22, 2004

[1] J. L. Drury, D. J. Mooney, *Biomaterials* **2003**, *24*, 4337.
[2] A. S. Hoffman, *Ann. N. Y. Acad. Sci.* **2001**, *944*, 62.
[3] D. L. Ellis, I. V. Yannas, *Biomaterials* **1996**, *17*, 291.
[4] T. D. Dziubla, M. C. Torjman, J. I. Joseph, M. Murphy-Tatum, A. M. Lowman, *Biomaterials* **2001**, *22*, 2893.
[5] M. H. Sheridan, L. D. Shea, M. C. Peters, D. J. Mooney, *J. Controlled Release* **2000**, *64*, 91.
[6] P. X. Ma, J. W. Choi, *Tissue Eng.* **2001**, *7*, 23.
[7] W. L. Murphy, R. G. Dennis, J. L. Kileny, D. J. Mooney, *Tissue Eng.* **2002**, *8*, 43.
[8] Q. P. Hou, D. W. Grijpma, J. Feijen, *J. Biomed. Mater. Res. Part B* **2003**, *67*, 732.
[9] L. Shapiro, S. Cohen, *Biomaterials* **1997**, *18*, 583.
[10] A. Blanco, E. Chomski, S. Grabtchak, M. Ibisate, S. John, S. W. Leonard, C. Lopez, F. Meseguer, H. Miguez, J. P. Mondia, G. A. Ozin, O. Toader, H. M. van Driel, *Nature* **2000**, *405*, 437.
[11] Y. N. Xia, B. Gates, Y. D. Yin, Y. Lu, *Adv. Mater.* **2000**, *12*, 693.
[12] A. Stein, *Microporous Mesoporous Mater.* **2001**, *44–45*, 227.
[13] P. Jiang, J. F. Bertone, V. L. Colvin, *Science* **2001**, *291*, 453.
[14] D. J. Irvine, A. Stachowiak, S. Jain, *Mater. Sci. Forum* **2003**, *426–432*, 3213.
[15] K. T. Nguyen, J. L. West, *Biomaterials* **2002**, *23*, 4307.
[16] K. S. Anseth, A. T. Metters, S. J. Bryant, P. J. Martens, J. H. Elisseeff, C. N. Bowman, *J. Controlled Release* **2002**, *78*, 199.
[17] M. P. Lutolf, G. P. Raeber, A. H. Zisch, N. Tirelli, J. A. Hubbell, *Adv. Mater.* **2003**, *15*, 888.
[18] B. D. Hughes, in *Random Walks and Random Environments*, Vol. 2, Clarendon Press, Oxford, U.K. **1996**, Ch. 1.
[19] J. Blease, J. W. Essam, C. M. Place, *Phys. Lett. A* **1976**, *57*, 199.
[20] S. F. Hulbert, F. A. Young, R. S. Mathews, J. J. Klawitter, C. D. Talbert, F. H. Stelling, *J. Biomed. Mater. Res.* **1970**, *4*, 433.
[21] S. R. Taylor, D. F. Gibbons, *J. Biomed. Mater. Res.* **1983**, *17*, 205.
[22] T. V. Chirila, I. J. Constable, G. J. Crawford, S. Vijayasekaran, D. E. Thompson, Y. C. Chen, W. A. Fletcher, B. J. Griffin, *Biomaterials* **1993**, *14*, 26.
[23] D. J. Mooney, D. F. Baldwin, N. P. Suh, J. P. Vacanti, R. Langer, *Biomaterials* **1996**, *17*, 1417.
[24] M. E. Gomes, A. S. Ribeiro, P. B. Malafaya, R. L. Reis, A. M. Cunha, *Biomaterials* **2001**, *22*, 883.
[25] L. J. Gibson, M. F. Ashby, in *Cellular Solids: Structure and Properties*, University Press, Cambridge, UK **1997**.
[26] M. M. Pradas, J. L. G. Ribelles, A. S. Aroca, G. G. Ferrer, J. S. Anton, P. Pissis, *Polymer* **2001**, *42*, 4667.
[27] Q. Liu, E. L. Hedberg, Z. W. Liu, R. Bahulekar, R. K. Meszlenyi, A. G. Mikos, *Biomaterials* **2000**, *21*, 2163.
[28] R. Barbucci, G. Leone, *J. Biomed. Mater. Res. Part B* **2004**, *68*, 117.
[29] A. Samani, J. Bishop, C. Luginbuhl, D. B. Plewes, *Phys. Med. Biol.* **2003**, *48*, 2183.
[30] W. C. Yeh, P. C. Li, Y. M. Jeng, H. C. Hsu, P. L. Kuo, M. L. Li, P. M. Yang, P. H. Lee, *Ultrasound Med. Biol.* **2002**, *28*, 467.
[31] E. Ruoslahti, M. D. Pierschbacher, *Science* **1987**, *238*, 491.
[32] D. L. Hern, J. A. Hubbell, *J. Biomed. Mater. Res.* **1998**, *39*, 266.
[33] S. F. Hossainy, J. A. Hubbell, *Biomaterials* **1994**, *15*, 921.
[34] *Poly(ethylene glycol): Chemistry and Biological Applications* (Eds: J. M. Harris, S. Zalipsky), American Chemical Society, Washington, DC **1997**.
[35] S. L. Riley, S. Dutt, R. De La Torre, A. C. Chen, R. L. Sah, A. Ratcliffe, *J. Mater. Sci. Mater. Med.* **2001**, *12*, 983.
[36] S. J. Bryant, R. J. Bender, K. L. Durand, K. S. Anseth, *Biotechnol. Bioeng.* **2004**, *86*, 747.
[37] M. A. Lichtman, *Exp. Hematol.* **1981**, *9*, 391.
[38] J. E. Gretz, A. O. Anderson, S. Shaw, *Immunol. Rev.* **1997**, *156*, 11.
[39] B. K. Mann, A. S. Gobin, A. T. Tsai, R. H. Schmedlen, J. L. West, *Biomaterials* **2001**, *22*, 3045.
[40] P. B. van Wachem, J. A. Plantinga, M. J. B. Wissink, R. Beernink, A. A. Poot, G. H. M. Engbers, T. Beugeling, *J. Biomed. Mater. Res.* **2001**, *55*, 368.

